Charge-independence breaking in the three-nucleon system

H. Witała,* W. Glöckle, and H. Kamada
Institut für Theoretische Physik, Ruhr-Universität Bochum, D-4630 Bochum, Germany
(Received 22 October 1990)

Charge-independence breaking is investigated theoretically and numerically in the three-nucleon ($3N$) system. Illustrations for the $3N$ bound states and for cross sections and spin observables in elastic nucleon-deuteron scattering and breakup processes are given, using exact solutions of the Faddeev equations with meson-theoretical $2N$ interactions.

I. INTRODUCTION

Charge-independence breaking (CIB) in the two-nucleon ($2N$) system is well established in the state $^1S_0$. The scattering lengths are -23.75 ± 0.01, -17.3 ± 0.8, and -18.5 ± 0.3 fm (Ref. 1) for the *np*, *pp* (with the Coulomb force extracted), and *nn* systems, respectively. Though the numbers for *pp* and *nn* may still have some small uncertainty, their significant difference to the *np* value is out of the question. That difference in scattering lengths carries over into a well-established difference of $^1S_0$ phase shifts for the *np* and *pp* systems.[2] Recent phase-shift analysis[3,4] also find significant CIB in the $^3P_0$,$^3P_1$, and $^3P_2$-$^3F_2$ states. In this work we want to study how strongly CIB affects $3N$ observables and how it has to be treated. Two possibilities exist: neutrons and protons are assumed either to be distinguishable or identical particles; in the latter case the space of states has to be enlarged by the isospin space. Assuming the neutrons and protons to be distinguishable, the three Faddeev equations for distinguishable particles reduce to two for the *nd* or *pd* systems; in the other case, the isospin violating $2N$ forces admix a state of total isospin $T=\frac{3}{2}$ to the dominant state $T=\frac{1}{2}$. To the best of our knowledge a detailed description of the transition between the two formalulations in the Faddeev formalism (and thereby the verification of their full equivalence) has not appeared in the literature. Therefore, we would like to lay out the two formulations and their equivalence in some detail in Sec. II. This will be carried through with modified Alt, Grassberger, and Sandhas (AGS) equations,[5] which we use so far in our numerical treatment of $3N$ scattering.[6] In Ref. 7 we have already regarded the question of incorporating CIB into our formalism, which led to the simple rule that the effective two-body t matrix in the state of isospin 1 and total $3N$ isospin $T=\frac{1}{2}$ is

$$t_{\rm eff}=\tfrac{2}{3}t_{nn(pp)}+\tfrac{1}{3}t_{np} \ . \tag{1.1}$$

That prescription has also been used in Ref. 8 for triton calculations and in a slightly more approximate manner in Ref. 9, where the $\frac{2}{3}-\frac{1}{3}$ mixture was applied on the level of $2N$ potentials (not t matrices).

The effects of CIB in the $3N$ system are of great interest. In triton they are clearly visible in the triton binding energy.[8,9,15] We illustrate that again in Sec. III for different meson-theoretical $2N$ interactions and 34 channel calculations. CIB is also visible in $3N$ scattering observables. A clear cut and important example is the region of $2N$ final-state interactions (FSI) in the $3N$ breakup process. Here the correct treatment of the different interactions in the $^1S_0$ $nn(pp)$ and *np* systems are very important. We study various breakup configurations in Sec. IV with respect to their sensitivity or nonsensitivity to CIB in the $^1S_0$ $2N$ force. We also clarify whether an approximate treatment of these effects in the form of the $\frac{2}{3}$-$\frac{1}{3}$ rule under the neglect of the $T=\frac{3}{2}$ states is thereby sufficient or whether the full complexity including the $T=\frac{3}{2}$ admixture is unavoidable.

In Ref. 10 we introduced a CIB of ^3P $2N$ interactions, which explained the persistent discrepancy between theory and experiment for the $3N$ analyzing power at low energies. Its effect on various breakup processes will also be investigated in Sec. IV.

Section V deals with elastic Nd scattering with the inclusion of many spin observables. Their sensitivity to CIB in the states $^1S_0$ and ^3P will be discussed. An important observable thereby is the analyzing power A_y. Our results are summarized in Sec. VI.

II. TREATMENT OF CHARGE-INDEPENDENCE BREAKING IN THE ISOSPIN FORMALISM FOR THREE NUCLEONS

If the neutron-neutron (or proton-proton) and neutron-proton interactions in the same orbital and spin angular-momentum states are different, one speaks of CIB. This is well established in the state $^1S_0$. There are also indications for CIB in the ^3P states.[2–4,10] Therefore, the correct treatment of the $3N$ system should consider neutrons and protons to be distinguishable, with the consequence of having two Faddeev equations for the *nd* or *pd* systems instead of one equation for identical particles. An alternative and fully equivalent formulation is based on the generalized Pauli principle. There the nucleons get additional isospin degrees of freedom and can

then be considered to be identical. As a consequence, their wave functions have to be antisymmetric under the exchange of any pair. In this section we want to explicitly lay out that isospin formulation and will show how the inclusion of the $T=\frac{3}{2}$ states in the *nd* and *pd* systems restore the dynamical difference between neutron-neutron (proton-proton) and neutron-proton pairs in the case of CIB. As will be shown in the next sections, for quite a few $3N$ observables, the neglection of the $T=\frac{3}{2}$ states is justified, though CIB effects are noticeable. In that case, the effective two-body t matrix (1.1) has to be used in the state $T=\frac{1}{2}$ with two-body isospin $t=1$, as will be shown below.

We begin our discussion by considering neutrons and protons to be distinguishable. For our notation we refer to Ref. 11. Let us regard the *nd* system as an example and let us enumerate the neutrons by one and two and the proton by three. Neutron-deuteron (*nd*) scattering is initiated by one of two channel states:

$$|\hat{\Phi}_1\rangle=|\varphi_d(23)\rangle|\mathbf{q}_0(1)\rangle\ ,\qquad |\hat{\Phi}_2\rangle=|\varphi_d(31)\rangle|\mathbf{q}_0(2)\rangle\ , \tag{2.1}$$

which are composed of a deuteron and a free neutron with relative momentum $\mathbf{q}_0$. The physical antisymmetrized $3N$ scattering state is

$$|\Psi^{(+)}\rangle=|\Psi_1^{(+)}\rangle-|\Psi_2^{(+)}\rangle\ , \tag{2.2}$$

where, in $|\Psi_i^{(+)}\rangle$, the neutron i is initially free. Then the operators $\tilde{U}$ for elastic and $\tilde{U}_3$ for rearrangement scattering are introduced by

$$(V_2+V_3)|\Psi^{(+)}\rangle\equiv U_{11}|\hat{\Phi}_1\rangle-U_{12}|\hat{\Phi}_2\rangle\equiv\tilde{U}|\hat{\Phi}_1\rangle\ , \tag{2.3}$$

$$(V_3+V_1)|\Psi^{(+)}\rangle=-\hat{P}_{12}(V_2+V_3)|\Psi^{(+)}\rangle=-\hat{P}_{12}\tilde{U}|\hat{\Phi}_1\rangle\ , \tag{2.4}$$

$$(V_1+V_2)|\Psi^{(+)}\rangle\equiv U_{31}|\hat{\Phi}_1\rangle-U_{32}|\hat{\Phi}_2\rangle\equiv\tilde{U}_3|\hat{\Phi}_1\rangle\ . \tag{2.5}$$

We used the standard "odd-man-out" notation for the pair interactions and the AGS transition operators $U_{\alpha\beta}$.[12] They obey the AGS equations[12]

$$U_{\alpha\beta}|\hat{\Phi}_\beta\rangle=(1-\delta_{\alpha\beta})G_0^{-1}|\hat{\Phi}_\beta\rangle+\sum_{\gamma\neq\alpha}t_\gamma G_0 U_{\gamma\beta}|\hat{\Phi}_\beta\rangle\ . \tag{2.6}$$

As a simple consequence of (2.6) we find

$$\tilde{U}|\hat{\Phi}_1\rangle=-\hat{P}_{12}G_0^{-1}|\hat{\Phi}_1\rangle-\hat{P}_{12}t_1G_0\tilde{U}|\hat{\Phi}_1\rangle+t_3G_0U_3|\hat{\Phi}_1\rangle\ , \tag{2.7}$$

$$\tilde{U}_3|\hat{\Phi}_1\rangle=(1-\hat{P}_{12})G_0^{-1}|\hat{\Phi}_1\rangle+(1-\hat{P}_{12})t_1G_0\tilde{U}|\hat{\Phi}_1\rangle\ . \tag{2.8}$$

Into these two coupled equations enter the *np* t operator $t_1\equiv t_{23}$ and the *nn* t operator $t_3\equiv t_{12}$, which are different for CIB.

The transition operator for the breakup process is

$$\sum_\alpha V_\alpha|\Psi^{(+)}\rangle=\sum_\alpha V_\alpha(|\Psi_1^{(+)}\rangle-|\Psi_2^{(+)}\rangle)\equiv U_{01}|\hat{\Phi}_1\rangle-U_{02}|\hat{\Phi}_2\rangle\equiv\tilde{U}_0|\hat{\Phi}_1\rangle\ . \tag{2.9}$$

Using the well-known[11] expressions

$$U_{0\alpha}|\hat{\Phi}_\alpha\rangle=\sum_\gamma t_\gamma G_0 U_{\gamma\alpha}|\hat{\Phi}_\alpha\rangle\ , \tag{2.10}$$

one easily finds

$$\tilde{U}_0|\hat{\Phi}_1\rangle=(1-\hat{P}_{12})t_1G_0\tilde{U}|\hat{\Phi}_1\rangle+t_3G_0\tilde{U}_3|\hat{\Phi}_1\rangle\ , \tag{2.11}$$

which expresses $\tilde{U}_0$ in terms of $\tilde{U}$ and $\tilde{U}_3$.

For the numerical performance it is advisable[5] to work with new operators $\tilde{T}$ and $\tilde{T}_3$ defined by

$$\tilde{U}_0\equiv(1-\hat{P}_{12})\tilde{T}+\tilde{T}_3\ , \tag{2.12}$$

which obviously obey the coupled set

$$\tilde{T}=-t_1\hat{P}_{12}+t_1G_0(-\hat{P}_{12}\tilde{T}+\tilde{T}_3)\ , \tag{2.13}$$

$$\tilde{T}_3=t_3(1-\hat{P}_{12})+t_3G_0(1-\hat{P}_{12})\tilde{T}\ . \tag{2.14}$$

This is the coupled set of equations[13] to which we shall compare the equations in the isospin formalism.

Once $\tilde{T}$ and $\tilde{T}_3$ are known, the operators for elastic and rearrangement processes follow by quadrature:

$$\tilde{U}=-\hat{P}_{12}G_0^{-1}-\hat{P}_{12}\tilde{T}+\tilde{T}_3\ , \tag{2.15}$$

$$\tilde{U}_3=(1-\hat{P}_{12})G_0^{-1}+(1-\hat{P}_{12})\tilde{T}\ . \tag{2.16}$$

Let us now regard the same physical situation of different *nn* and *np* forces in the isospin formalism. In the *nd* system there are three charge states

$$|n(2)p(3)n(1)\rangle\ ,\quad |p(2)n(3)n(1)\rangle\ ,\quad |n(2)n(3)p(1)\rangle\ . \tag{2.17}$$

We shall drop the particle numbers in the following. Our convention is that the neutron (proton) carries the z component $\frac{1}{2}$ $(-\frac{1}{2})$ of the isospin. Then the three $\frac{1}{2}$ nucleons can be coupled to total isospin $T=\frac{1}{2}$ and $\frac{3}{2}$ states

$$|(t\tfrac{1}{2})TM_T=\tfrac{1}{2}\rangle\ . \tag{2.18}$$

These are again three states with two-body isospins $t=0$, 1 for $T=\frac{1}{2}$, and $t=1$ for $T=\frac{3}{2}$. The convention is that t refers to the 2-3 subsystem and $\frac{1}{2}$ to particle 1. The connection between (2.17) and (2.18) is

$$|(0\tfrac{1}{2})\tfrac{1}{2}\,\tfrac{1}{2}\rangle=\frac{1}{\sqrt{2}}(|npn\rangle-|pnn\rangle)\ , \tag{2.19}$$

$$|(1\tfrac{1}{2})\tfrac{1}{2}\,\tfrac{1}{2}\rangle=\sqrt{2/3}|nnp\rangle-\frac{1}{\sqrt{6}}(|npn\rangle+|pnn\rangle)\ , \tag{2.20}$$

$$|(1\tfrac{1}{2})\tfrac{3}{2}\,\tfrac{1}{2}\rangle=\frac{1}{\sqrt{3}}(|nnp\rangle+|npn\rangle+|pnn\rangle)\ , \tag{2.21}$$

or

$$|pnn\rangle = -\frac{1}{\sqrt{2}}|(0\tfrac{1}{2})\tfrac{1}{2}\tfrac{1}{2}\rangle - \frac{1}{\sqrt{6}}|(1\tfrac{1}{2})\tfrac{1}{2}\tfrac{1}{2}\rangle + \frac{1}{\sqrt{3}}|(1\tfrac{1}{2})\tfrac{3}{2}\tfrac{1}{2}\rangle , \quad (2.22)$$

$$|npn\rangle = \frac{1}{\sqrt{2}}|(0\tfrac{1}{2})\tfrac{1}{2}\tfrac{1}{2}\rangle - \frac{1}{\sqrt{6}}|(1\tfrac{1}{2})\tfrac{1}{2}\tfrac{1}{2}\rangle + \frac{1}{\sqrt{3}}|(1\tfrac{1}{2})\tfrac{3}{2}\tfrac{1}{2}\rangle , \quad (2.23)$$

$$|nnp\rangle = \sqrt{2/3}|(1\tfrac{1}{2})\tfrac{1}{2}\tfrac{1}{2}\rangle + \frac{1}{\sqrt{3}}|(1\tfrac{1}{2})\tfrac{3}{2}\tfrac{1}{2}\rangle . \quad (2.24)$$

We recognize that if we want to choose particles 2 and 3 to be specific nucleons, we need the total isospin $T=\frac{3}{2}$. In the identical particle formalism this case occurs automatically and the absence of $T=\frac{3}{2}$ reflects either the dynamical equivalence of *nn* and *np* pairs or an approximation, whose quality depends on the amount of CIB.

Similarly the $T=\frac{1}{2}$ and $\frac{3}{2}$ states are needed to distinguish the *nn* and *np* t matrices in the $3N$ system. We regard the $2N$ t operators in the three-particle isospin space assuming, of course, charge conservation:

$$\langle (t\tfrac{1}{2})TM_T|t|(t'\tfrac{1}{2})T'M'_T\rangle = \delta_{M_T M'_T} \times \sum_{\nu} C(t\tfrac{1}{2}T,\nu M_T-\nu) \times C(t'\tfrac{1}{2}T',\nu M_T-\nu) \times \langle t\nu|t|t'\nu\rangle . \quad (2.25)$$

The $2N$ t operator conserves the isospin t to a high degree of accuracy but depends on the charge states of the two interacting nucleons. One finds from (2.25)

$$\langle (0\tfrac{1}{2})\tfrac{1}{2}\tfrac{1}{2}|t|(0\tfrac{1}{2})\tfrac{1}{2}\tfrac{1}{2}\rangle = t_{np}^{t=0} , \quad (2.26)$$

$$\langle (1\tfrac{1}{2})\tfrac{1}{2}\tfrac{1}{2}|t|(1\tfrac{1}{2})\tfrac{1}{2}\tfrac{1}{2}\rangle = \tfrac{2}{3}t_{nn}^{t=1} + \tfrac{1}{3}t_{np}^{t=1} , \quad (2.27)$$

$$\langle (1\tfrac{1}{2})\tfrac{1}{2}\tfrac{1}{2}|t|(1\tfrac{1}{2})\tfrac{3}{2}\tfrac{1}{2}\rangle = \langle (1\tfrac{1}{2})\tfrac{3}{2}\tfrac{1}{2}|t|(1\tfrac{1}{2})\tfrac{1}{2}\tfrac{1}{2}\rangle = \frac{\sqrt{2}}{3}(t_{nn}^{t=1}-t_{np}^{t=1}) , \quad (2.28)$$

$$\langle (1\tfrac{1}{2})\tfrac{3}{2}\tfrac{1}{2}|t|(1\tfrac{1}{2})\tfrac{3}{2}\tfrac{1}{2}\rangle = \tfrac{1}{3}t_{nn}^{t=1} + \tfrac{2}{3}t_{np}^{t=1} . \quad (2.29)$$

In obvious notations we introduced the two-body t matrices for the *nn* and *np* systems in the isospin states $t=0$ and 1. We explicitly see the need of the $T=\frac{3}{2}$ state to distinguish between the $t_{np}^{t=1}$ and $t_{nn}^{t=1}$ interactions:

$$t_{nn}^{t=1} = \langle (1\tfrac{1}{2})\tfrac{1}{2}\tfrac{1}{2}|t|(1\tfrac{1}{2})\tfrac{1}{2}\tfrac{1}{2}\rangle + \frac{1}{\sqrt{2}}\langle (1\tfrac{1}{2})\tfrac{3}{2}\tfrac{1}{2}|t|(1\tfrac{1}{2})\tfrac{1}{2}\tfrac{1}{2}\rangle , \quad (2.30)$$

$$t_{np}^{t=1} = \langle (1\tfrac{1}{2})\tfrac{1}{2}\tfrac{1}{2}|t|(1\tfrac{1}{2})\tfrac{1}{2}\tfrac{1}{2}\rangle - \sqrt{2}\langle (1\tfrac{1}{2})\tfrac{3}{2}\tfrac{1}{2}|t|(1\tfrac{1}{2})\tfrac{1}{2}\tfrac{1}{2}\rangle . \quad (2.31)$$

A decomposition analogous to (2.25) is valid for the two-body potential V:

$$\langle (t\tfrac{1}{2})TM_T=\tfrac{1}{2}|V|(t'\tfrac{1}{2})T'M_T=\tfrac{1}{2}\rangle = \delta_{tt'}\delta_{TT'}\delta_{T1/2}[\delta_{t0}V_{np}^{t=0}+\delta_{t1}(\tfrac{2}{3}V_{nn}^{t=1}+\tfrac{1}{3}V_{np}^{t=1})] + \delta_{tt'}\delta_{t1}(1-\delta_{TT'})\frac{\sqrt{2}}{3}(V_{nn}^{t=1}-V_{np}^{t=1}) + \delta_{tt'}\delta_{t1}\delta_{TT'}\delta_{T3/2}(\tfrac{1}{3}V_{nn}^{t=1}+\tfrac{2}{3}V_{np}^{t=1}) . \quad (2.32)$$

The t and V operators are connected by the Lippmann-Schwinger equation

$$t = V + VG_0 t . \quad (2.33)$$

In case of CIB in the state $t=1$ it is a coupled set of two equations ($T=\frac{1}{2},\frac{3}{2}$, T' fixed):

$$\langle (1\tfrac{1}{2})TM_T|t|(1\tfrac{1}{2})T'M_T\rangle = \langle (1\tfrac{1}{2})TM_T|V|(1\tfrac{1}{2})T'M_T\rangle + \sum_{T''=1/2,3/2}\langle (1\tfrac{1}{2})TM_T|V|(1\tfrac{1}{2})T''M_T\rangle G_0\langle (1\tfrac{1}{2})T''M_T|t|(1\tfrac{1}{2})T'M_T\rangle . \quad (2.34)$$

Inserting the decomposition (2.32) for V, it can easily be shown that the linear combinations (2.26)–(2.29) are the solutions. Thereby, $t_{nn}^{t=1}$ and $t_{np}^{t=1}$ obey uncoupled (in isospin) Lippmann-Schwinger equations driven by $V_{nn}^{t=1}$ and $V_{np}^{t=1}$, respectively. Based on that introduction, we can regard the modified AGS equation[5]

$$T = tP + tPG_0T \quad (2.35)$$

valid for identical particles. In Ref. 7 we projected (2.35) onto two types of basis states:

$$|pq\alpha\rangle \equiv |pq \text{ angular momenta}\rangle|(t\tfrac{1}{2})T=\tfrac{1}{2}M_T\rangle , \quad (2.36)$$

$$|pq\beta\rangle \equiv |pq \text{ angular momenta}\rangle|(t\tfrac{1}{2})T=\tfrac{3}{2}M_T\rangle . \quad (2.37)$$

If the transition matrix elements (2.28) are different from zero, the amplitudes $\langle pq\alpha|T|\Phi\rangle$ and $\langle pq\beta|T|\Phi\rangle$ are coupled. It is that set of equations which we solve if the distinction between the *nn* and *np* forces has noticeable effects for certain $3N$ observables. In case the neglection of $T=\frac{3}{2}$ states is justified, CIB is taken care of by the effective two-body t matrix shown in Sec. I and Eq. (2.27).

Now we want to demonstrate that (2.35) is equivalent to the two coupled equations (2.13) and (2.14) if we assume that the *nn* and *np* $t=1$ forces are different.

The initial channel state $|\hat{\Phi}\rangle \equiv |\hat{\Phi}_1\rangle$ is enriched by a $3N$ isospin state

$$|\Phi\rangle = \hat{P}_0 |\hat{\Phi}\rangle |(0\tfrac{1}{2})\tfrac{1}{2}\tfrac{1}{2}\rangle \ . \tag{2.38}$$

For convenience we made the symmetry of $|\hat{\Phi}\rangle$ in momentum and spin space explicit by introducing

$$\hat{P}_0 \equiv \tfrac{1}{2}(1+\hat{P}_{23}) \ . \tag{2.39}$$

The caret indicates, as previously, only the operations onto degrees of freedom in momentum and spin space.

Next we evaluate $P|\Phi\rangle$, where P is the sum of two cyclical permutation operators (acting on all degrees of freedom):

$$\begin{aligned} P|\Phi\rangle &\equiv (P_{12}P_{23}+P_{13}P_{23})|\Phi\rangle \\ &= \frac{1}{\sqrt{2}}(|nnp\rangle - |npn\rangle)\hat{P}_{12}\hat{P}_{23}\hat{P}_0|\hat{\Phi}\rangle \\ &\quad + \frac{1}{\sqrt{2}}|pnn\rangle - |nnp\rangle)\hat{P}_{13}\hat{P}_{23}\hat{P}_0|\hat{\Phi}\rangle \ . \end{aligned} \tag{2.40}$$

Introducing

$$\hat{P}_1 \equiv \tfrac{1}{2}(1-\hat{P}_{23}) \ , \tag{2.41}$$

one finds

$$\begin{aligned} P|\Phi\rangle &= \frac{1}{\sqrt{2}}|nnp\rangle 2\hat{P}_1\hat{P}_{12}\hat{P}_0|\hat{\Phi}\rangle \\ &\quad - \frac{1}{\sqrt{2}}(|npn\rangle + |pnn\rangle)\hat{P}_1\hat{P}_{12}\hat{P}_0|\hat{\Phi}\rangle \\ &\quad - \frac{1}{\sqrt{2}}(|npn\rangle - |pnn\rangle)\hat{P}_0\hat{P}_{12}\hat{P}_0|\hat{\Phi}\rangle \ . \end{aligned} \tag{2.42}$$

The t operator given in (2.26)–(2.29) can be equivalently represented as

$$\begin{aligned} t &= |nn\rangle t_{nn}^{t=1}\langle nn| \\ &\quad + \tfrac{1}{2}(|np\rangle + |pn\rangle)t_{np}^{t=1}(\langle np| + \langle pn|) \\ &\quad + \tfrac{1}{2}(|np\rangle - |pn\rangle)t_{np}^{t=0}(\langle np| - \langle pn|) \ . \end{aligned} \tag{2.43}$$

Consequently,

$$\begin{aligned} tP|\Phi\rangle &= \sqrt{2}|nnp\rangle t_{nn}^{t=1}\hat{P}_1\hat{P}_{12}\hat{P}_0|\hat{\Phi}\rangle \\ &\quad - \frac{1}{\sqrt{2}}(|npn\rangle + |pnn\rangle)t_{np}^{t=1}\hat{P}_1\hat{P}_{12}\hat{P}_0|\hat{\Phi}\rangle \\ &\quad - \frac{1}{\sqrt{2}}(|npn\rangle - |pnn\rangle)t_{np}^{t=0}\hat{P}_0\hat{P}_{12}\hat{P}_0|\hat{\Phi}\rangle \ . \end{aligned} \tag{2.44}$$

Now let us regard the coupled set resulting from projecting (2.35) onto the basis states (2.36) and (2.37). We can form linear combinations (2.23) such that one projects by $\langle npn|$. This leads to the driving term

$$\langle npn|tP|\Phi\rangle = -\frac{1}{\sqrt{2}}(t_{np}^{t=1}\hat{P}_1 + t_{np}^{t=0}\hat{P}_0)\hat{P}_{12}\hat{P}_0|\hat{\Phi}\rangle \ . \tag{2.45}$$

The expression in the bracket is the full t operator for the np system:

$$t_{np} \equiv t_{np}^{t=1}\hat{P}_1 + t_{np}^{t=0}\hat{P}_0 \ . \tag{2.46}$$

We see that $t^{t=1}$ ($t^{t=0}$) acts on antisymmetric (symmetric) states in momentum and spin space, as it should. So we end up with the driving term

$$\langle npn|tP|\Phi\rangle = -\frac{1}{\sqrt{2}}t_{np}(23)\hat{P}_{12}\hat{P}_0|\hat{\Phi}\rangle \ . \tag{2.47}$$

For the sake of clarity, we indicated the particle numbers again. Now we regard the second term on the right-hand side of (2.35) and find after some simple algebra

$$\begin{aligned} \langle npn|tPG_0T|\Phi\rangle &= \tfrac{1}{2}t_{np}^{t=1}G_0(\hat{P}_{12}\hat{P}_{23}\langle pnn| + \hat{P}_{13}\hat{P}_{23}\langle npn|)T|\Phi\rangle + \tfrac{1}{2}t_{np}^{t=1}G_0(\hat{P}_{12}\hat{P}_{23}+\hat{P}_{13}\hat{P}_{23})\langle nnp|T|\Phi\rangle \\ &\quad + \tfrac{1}{2}t_{np}^{t=0}G_0(\hat{P}_{12}\hat{P}_{23}\langle pnn| - \hat{P}_{13}\hat{P}_{23}\langle npn|)T|\Phi\rangle + \tfrac{1}{2}t_{np}^{t=0}G_0(-\hat{P}_{12}\hat{P}_{23}+\hat{P}_{13}\hat{P}_{23})\langle nnp|T|\Phi\rangle \ . \end{aligned} \tag{2.48}$$

The amplitude $T|\Phi\rangle$ is antisymmetric in particles 2 and 3. This follows from the antisymmetry of $|\Phi\rangle$. Namely, the driving term of (2.35) is antisymmetric,

$$\begin{aligned} P_{23}tP|\Phi\rangle &= t(23)P_{23}P|\Phi\rangle \\ &= t(23)PP_{23}|\Phi\rangle = -tP|\Phi\rangle \ , \end{aligned} \tag{2.49}$$

and (2.35) is linear. Consequently,

$$P_{23}T|\Phi\rangle = -T|\Phi\rangle \tag{2.50}$$

and, therefore,

$$\hat{P}_{23}\langle nnp|T|\Phi\rangle = -\langle nnp|T|\Phi\rangle \ , \tag{2.51}$$

$$\hat{P}_{23}\langle pnn|T|\Phi\rangle = -\langle npn|T|\Phi\rangle \ . \tag{2.52}$$

This will now be used to simplify the right-hand side of (2.48):

$$\begin{aligned} (\mp\hat{P}_{12}\hat{P}_{23}+\hat{P}_{13}\hat{P}_{23})\langle nnp|T|\Phi\rangle &= (\mp\hat{P}_{23}\hat{P}_{13}\hat{P}_{23}\hat{P}_{23}+\hat{P}_{13}\hat{P}_{23})\langle nnp|T|\Phi\rangle \\ &= (1\pm\hat{P}_{23})\hat{P}_{13}\hat{P}_{23}\langle nnp|T|\Phi\rangle \ , \end{aligned} \tag{2.53}$$

$$\hat{P}_{12}\hat{P}_{23}\langle pnn|T|\Phi\rangle \mp \hat{P}_{13}\hat{P}_{23}\langle npn|T|\Phi\rangle = -\hat{P}_{12}\langle npn|T|\Phi\rangle \mp \hat{P}_{23}\hat{P}_{12}\langle npn|T|\Phi\rangle$$
$$= -(1\pm\hat{P}_{23})\hat{P}_{12}\langle npn|T|\Phi\rangle \ . \tag{2.54}$$

Using (2.46) one gets

$$\langle npn|T|\Phi\rangle = -\frac{1}{\sqrt{2}}t_{np}(23)\hat{P}_{12}\hat{P}_0|\hat{\Phi}\rangle + t_{np}(23)G_0\hat{P}_{13}\hat{P}_{23}\langle nnp|T|\Phi\rangle - t_{np}(23)G_0\hat{P}_{12}\langle npn|T|\Phi\rangle \ . \tag{2.55}$$

At this stage we arrived at amplitudes and operators which refer to neutrons and protons carrying numbers. Therefore, we can compare with Eq. (2.13). We recovered exactly that form and can identify

$$\langle npn|T|\Phi\rangle = \tilde{T}|\hat{\Phi}\rangle\frac{1}{\sqrt{2}} \ , \tag{2.56}$$

$$\hat{P}_{13}\hat{P}_{23}\langle nnp|T|\Phi\rangle = \tilde{T}_3|\hat{\Phi}\rangle\frac{1}{\sqrt{2}} \ . \tag{2.57}$$

The factor $1/\sqrt{2}$ arises from the normalization of the isospin state (2.19).

The equation for $\hat{P}_{13}\hat{P}_{23}\langle nnp|T|\Phi\rangle$ remains to be worked out. Similar steps, sketched in the Appendix, lead from (2.35) to

$$\hat{P}_{13}\hat{P}_{23}\langle nnp|T|\Phi\rangle = \frac{1}{\sqrt{2}}t_{nn}^{t=1}(12)(1-\hat{P}_{12})\hat{P}_0|\hat{\Phi}\rangle + t_{nn}^{t=1}(12)G_0(1-\hat{P}_{12})\langle npn|T|\Phi\rangle \ . \tag{2.58}$$

This is the second equation (2.14) in the coupled set (2.13) and (2.14). This concludes the demonstration of the equivalence of (2.35)—with the understanding that the $T=\frac{1}{2}$ and $\frac{3}{2}$ states are used—to the coupled set (2.13) and (2.14).

III. CHARGE-INDEPENDENCE BREAKING IN THE TRITON

The fact that the np force is slightly stronger than the nn force in the state $^1S_0$ leads to a correction to the theoretical triton binding energies, which are calculated with only one type of $2N$ force. So the pure Paris,[14] Bonn,[15] Nijmegen,[16] Argonne,[17] Reid,[18] etc. potential predictions have to be modified. Studies of that type have already been undertaken[8,9,15,19] leading to shifts of about 100–200 keV. We would like to illustrate that again for the meson-theoretical $2N$ interactions from the Paris and Bonn groups. Therefore, we include the $T=\frac{3}{2}$ admixture, which was neglected in Refs. 8, 9, and 15.

We use our momentum-space code[20] including 34 channels. The results for the Paris, Bonn A,[15] and Bonn B (Ref. 15) potentials are displayed in Table I. They agree very well with previous results.[8,9,21] Now we include CIB in the $^1S_0$ state. First we neglect the $T=\frac{3}{2}$ admixture and incorporate CIB only through the effective t operator, Eq. (2.1), in the $^1S_0$ state. For the Paris calculation, t_{nn} is taken from the Paris potential (neglecting charge-symmetry breaking) and t_{np} from Bonn B. The remaining t matrices are taken from the Paris potential. For the Bonn A and Bonn B calculations, t_{nn} is taken from Bonn B with the σ-meson coupling constant modified to $g_\sigma^2/4\pi=8.8557$,[15] which adjusts the $^1S_0$ $2N$ force to the pp system, and t_{np} is taken either from Bonn A or Bonn B. All the remaining t matrices are either from Bonn A or Bonn B, respectively. The resulting binding energies are displayed in the second row of Table I. We see the expected shifts, downward in the case of the Paris potential and upward in the case of the Bonn potentials. The Paris and Bonn B potentials have similar strengths in the $^3S_1$-$^3D_1$ tensor force, which is measured in the similar ε_1 mixing parameter and the similar deuteron d-state probability $P_d=5.77\%$ (Paris) and $P_d=4.99\%$ (Bonn B). Now correcting for the different $^1S_0$ forces for np and nn (pp) pairs, we see that these two potentials come closer to each other in the predictions of the triton binding energy. On the other hand, the Bonn A potential with a significantly weaker tensor force (smaller ε_1 and smaller $P_d=4.38\%$) binds the triton stronger and, correcting for the $^1S_0$ forces, the result is still closer to the experimental value of -8.48 MeV than for the Paris and Bonn B potentials.

Let us now include the $T=\frac{3}{2}$ admixture. The Faddeev equation reads

$$\psi = G_0 tP\psi \ . \tag{3.1}$$

If we assume that only $t(^1S_0)$ breaks CI, one more "channel" is added to the, by now, standard 34 angular momenta and isospin combinations. The jJ coupling basis states in momentum space are

$$|pq(ls)j(\lambda\tfrac{1}{2})J\mathcal{J}(t\tfrac{1}{2})T\rangle \ , \tag{3.2}$$

where $(ls)j$ and isospin t refer to the two-body subsystem and $(\lambda\frac{1}{2})J$ to the third particle. $\mathcal{J}$ and T are the total angular momentum and isospin of the triton and p,q standard Jacobi momenta. CIB in the $^1S_0$ state ($l=s=j=0$) adds to the standard "channel"

$$|pq(00)0(0\tfrac{1}{2})\tfrac{1}{2}\mathcal{J}=\tfrac{1}{2}(1\tfrac{1}{2})T=\tfrac{1}{2}\rangle \ , \tag{3.3}$$

TABLE I. Triton binding energies for three potentials. First row: 34-channel calculations. Second row: CIB in $^1S_0$ included via t_{eff} of (1.1), $T=\frac{3}{2}$ neglected. Third row: CIB in $^1S_0$ treated exactly including $T=\frac{3}{2}$. Change in energy in the fourth digit not shown.

	Paris	Bonn A	Bonn B
E (MeV)	−7.46	−8.32	−8.14
	−7.59	−8.08	−7.92
	−7.59	−8.08	−7.92

TABLE II. Artificial strength parameters from Ref. 10 modifying the Bonn B potential in the ^3P states.

	λ_{pp}	λ_{np}	λ_{nn}
$^3P_0$	0.86	1.04	0.75
$^3P_1$	1.05	1.07	1.08
$^3P_2$-$^3F_2$	1.02	1.03	1.03

the additional one

$$|pq(00)0(0\tfrac{1}{2})\tfrac{1}{2}\mathcal{A}=\tfrac{1}{2}(1\tfrac{1}{2})T=\tfrac{3}{2}\rangle \ . \tag{3.4}$$

The resulting binding energies are shown in the third row of Table I. As expected in Refs. 8 and 9, the effect of including $T=\frac{3}{2}$ in the triton binding energy is very small. (We estimate it to be 1 keV.)

Finally, we study CIB in the ^3P $2N$ forces. In Ref. 10 we found that the experimental np and pp analyzing powers A_y allowed for ^3P phase shifts, which are different for the np and pp systems. We generated these new ^3P phases by modifying the Bonn B potential in the ^3P states. This was done by introducing artificial strength parameters into the Bonn B $2N$ potential. They are displayed in Table II. The modified Bonn B potential describes the experimental analyzing powers in the pd system rather well—contrary to all previous trials with standard $2N$ potentials. In order to also describe the nd data for A_y we had to introduce charge-symmetry breaking. The corresponding strength parameters λ_{nn} in the ^3P states are also shown in Table II. This defines the Bonn B potential modified in the states ^3P as we used it for triton calculations. We applied t_{eff} of (1.1) for the ^3P states and the state $^1S_0$, neglecting in both cases the $T=\frac{3}{2}$ admixtures. The result is -7.89 MeV for the Bonn B potential. The effect is very small, as could be expected from the small contribution of ^3P $2N$ forces to the triton binding energy. For the binding-energy difference of ^{3}He and ^{3}H, however, which is not fully explained by the Coulomb force,[8] an effect of charge-symmetry breaking in ^3P states may be visible. For the phenomenological Bonn B potentials modified in ^3P states according to Table II, the binding-energy differences between ^{3}H and ^{3}He are $E_{^3\text{H}}-E_{^3\text{He}}=10$ keV. That difference is only due to the Bonn B modifications in the ^3P states as given in Table II. (In the $^1S_0$ state, charge symmetry is assumed.) That small effect of 10 keV reduces the energetic distance between the (negative) binding energies of ^{3}H and ^{3}He and opposes the effect of charge-symmetry breaking in the state $^1S_0$. In Ref. 10 we assumed that the difference between the low-energy pd and nd analyzing powers in the maxima are caused by CSB in the ^3P states. In case part of it, or even all, is caused by the Coulomb force acting in the pd system, CSB can be reduced and, consequently, our result of 10 keV will decrease, too.

IV. EFFECTS OF CHARGE-INDEPENDENCE BREAKING IN THE Nd BREAKUP PROCESS

We solved Eq. (2.35) for the Bonn B potential acting in all $2N$ states with $j\leq 3$. In the $^1S_0$ state we either used the original Bonn B potential, which is adjusted to the np system, or a version which is adjusted to the pp system. This is reflected in two different coupling constants as mentioned in Sec. III. In this work we neglect charge-symmetry breaking in the $^1S_0$ state and identify the pp and nn interactions. We shall display the results of four different dynamical assumptions for the forces in the $^1S_0$ state: a pure Bonn $B\equiv$Bonn B (np) calculation, with np forces between all $2N$ pairs, a pure Bonn B (pp) calculation, with pp ($=nn$) forces between all $2N$ pairs, CIB in the $T=\frac{1}{2}$ state, with t_{eff} between all $2N$ pairs, and CIB in the $T=\frac{1}{2}$ and $\frac{3}{2}$ state, with the proper np and nn ($=pp$) forces.

Out of the rich spectrum of breakup configurations we selected a few which were suggested to be especially interesting in the search for three-nucleon force (3NF) effects.[22] These are the space-star, the collinear, the quasifree scattering (QFS), and final-state interaction configurations. We want to investigate in how far the exact treatment of CIB in these configurations is of importance or whether the $\frac{2}{3}$-$\frac{1}{3}$ rule of Eq. (1.1) neglecting $T=\frac{3}{2}$ is sufficient.

From the Watson-Migdal approximation[23] and $3N$ calculations with the Paris and Bonn potentials[24,7] it is well

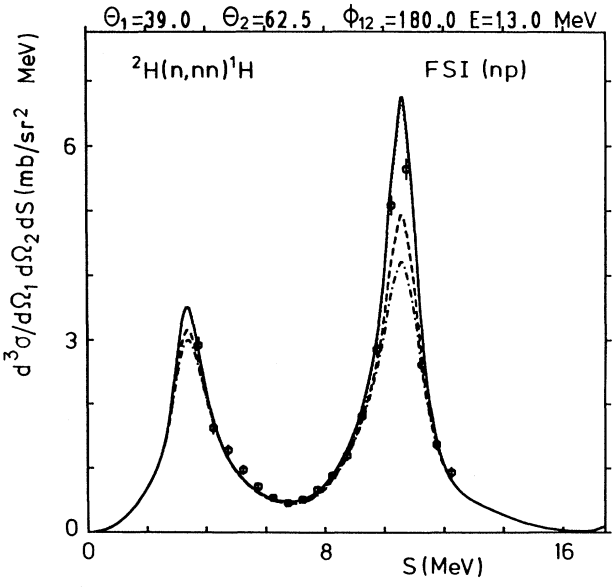

FIG. 1. The cross section $d^3\sigma/d\Omega_1 d\Omega_2 dS$ as a function of arc length S for the np FSI configuration at $\Theta_1=39.0°$, $\Theta_2=62.5°$, and $\Phi_{12}=180°$. Experimental data are from Ref. 25. The theoretical curves are the Bonn B potential predictions, with two-nucleon interactions restricted to act in the partial-wave states $j\leq 3$ and with a different $^1S_0$ dynamic: the dotted and dash-dotted curves result if the $^1S_0$ forces of Bonn B (np) and Bonn B (pp) are used, respectively; the $T=\frac{1}{2}$ approximation in the form of the $\frac{2}{3}$-$\frac{1}{3}$ rule using these $^1S_0$ forces and the full calculation with $T=\frac{3}{2}$ admixture are given by dashed and continuous curves, respectively.

known that the FSI peak area is strongly dependent on the $^1S_0$ scattering length. This is visible in Figs. 1 and 2, where *np* and *nn* FSI configurations at $E_n^{\rm lab}=13.0$ MeV are shown. The curves for the Bonn *B* (*np*) and Bonn *B* (*pp*) potentials are indeed far apart in the FSI peak areas. The Bonn *B* (*np*) curve corresponding to the scattering length a_{np} ($^1S_0$) $=-23.76$ fm lies higher than the Bonn *B* (*pp*) curve corresponding to a_{pp} ($^1S_0$) $=-17.66$ fm. The $T=\frac{1}{2}$ approximation ($\frac{2}{3}$-$\frac{1}{3}$ rule) lies in between. The full calculation including $T=\frac{3}{2}$, which distinguishes between the *np* and *nn* forces, coincides—to our surprise—very well with the respective pure potential predictions. It seems unavoidable to conclude that the full breakup amplitude has the structure of a production amplitude for the pair interacting in the final state multiplied by an amplitude which is responsible for the FSI per se. The first amplitude should then be insensitive to CIB, while all the sensitivity should be carried by the second one. This deserves further theoretical investigation. We conclude that, in the whole FSI peak area, the full treatment of CIB in the form of the $T=\frac{3}{2}$ admixture is necessary. The $T=\frac{1}{2}$ approximation in the form of the $\frac{2}{3}$-$\frac{1}{3}$ rule is inadequate. An alternative is to perform two calculations with pure potentials adapted to the pair of nucleons interacting in the final state. The good agreement of the *nd* data[25] with the full calculation as seen in Fig. 1 might be fortuitous, since our theory has not yet been folded with energy and angular resolutions.

The collinear configuration in the cases we studied turned out to be insensitive to CIB. We show an example in Fig. 3, where the four curves at the collinearity point overlap. The nearby peaks are slopes of FSI's from neighboring angles. In the right peak, CIB effects are strongly visible and the $T=\frac{3}{2}$ admixture is essential. It is a *np* FSI. Here we also show *nd* data[25] which, at and around the collinearity condition, deviate significantly from theory. We feel that a second independent measurement should confirm the data before a signature for dynamics beyond the $2N$ forces only can be claimed. The agreement in the FSI peak area may again be fortuitous, since we have not yet corrected the results for experimental resolutions.

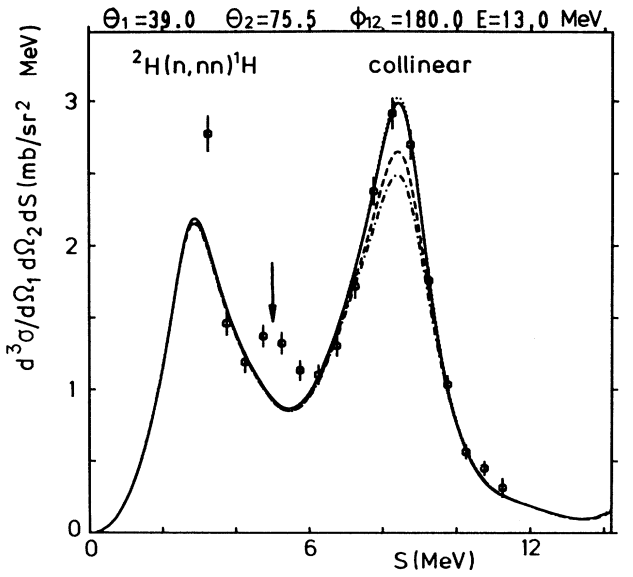

FIG. 3. The same as in Fig. 1 for the collinear configuration at $\Theta_1=39.0°$, $\Theta_2=75.5°$, and $\Phi_{12}=180°$. The collinearity point is indicated by the arrow.

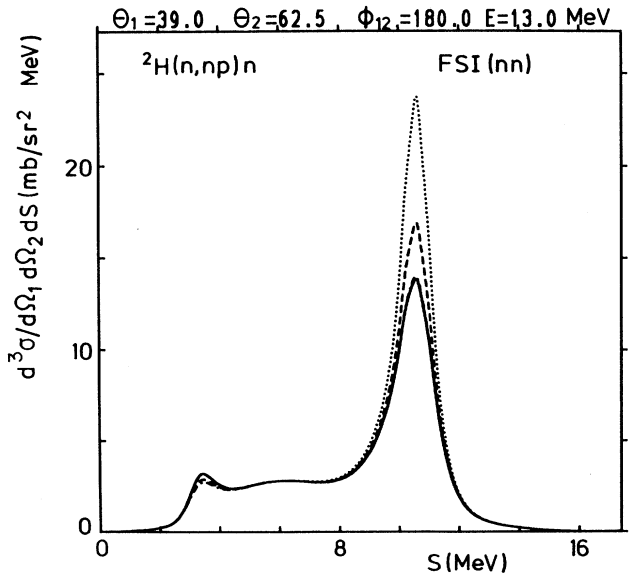

FIG. 2. The same as in Fig. 1 for the *nn* FSI configuration at $\Theta_1=39.0°$, $\Theta_2=62.5°$, and $\Phi_{12}=180°$.

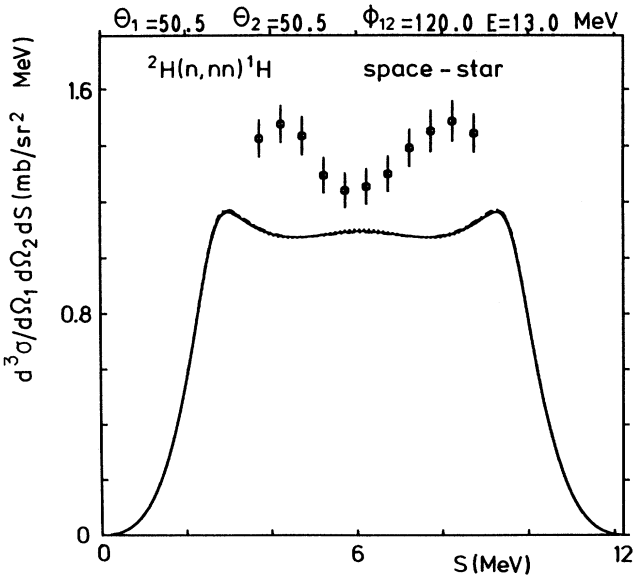

FIG. 4. The same as in Fig. 1 for the space-star configuration at $\Theta_1=\Theta_2=50.5°$ and $\Phi_{12}=120°$.

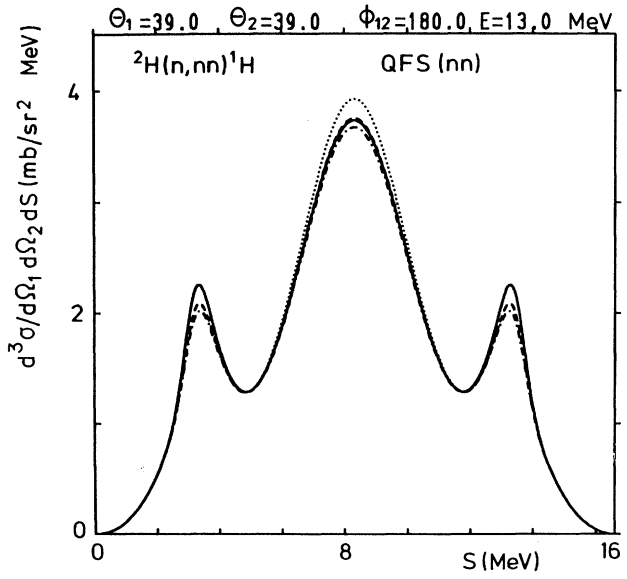

FIG. 5. The same as in Fig. 1 for the QFS (*nn*) configuration at $\Theta_1=\Theta_2=39.0°$ and $\Phi_{12}=180°$.

Another configuration besides collinearity which is robust against changes in $2N$ dynamics is the space star. In Fig. 4 we show results at $E_n^{\rm lab}=13.0$ MeV. The four curves overlap totally. This is in line with the result[26] that the exchange of the Bonn A against the Paris potential shifts the cross section only by $\approx 4\%$. Therefore, like collinearity, the space star is an ideal candidate to look for $3NF$ effects. The *nd* data[25] at 13.0 MeV show a strong variation along the S curve which is not present in theory. They should also be confirmed by a second independent measurement before a signature for 3NF effects can be claimed.

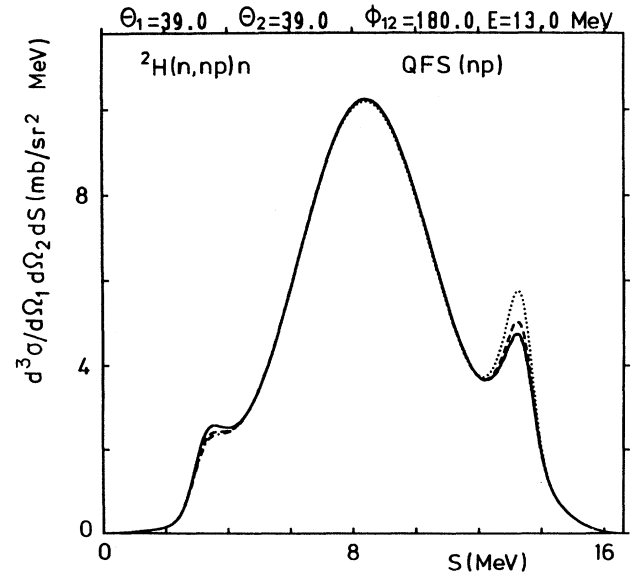

FIG. 6. The same as in Fig. 1 for the QFS (*np*) configuration at $\Theta_1=\Theta_2=39.0°$ and $\Phi_{12}=180°$.

In Figs. 5 and 6 we show *nn* and *np* QFS's at $E_n^{\rm lab}=13.0$ MeV. In the whole peak area (central peak) the difference between the approximate calculation ($T=\frac{1}{2}$ only) and the result of the full calculation (inclusion of $T=\frac{3}{2}$) is negligible. For the *np* QFS even the predictions of the pure potentials coincide with each other and the full calculation.

Finally, let us regard a possible CIB in the ^3P states as discussed in Sec. III. The effects on the breakup cross sections shown in Figs. 1–6 are totally negligible except for the *np* QFS (and the two FSI's), where the $T=\frac{3}{2}$ admixture decreases (increases) the cross section by $\sim 3\%$ in comparison to the results based on pure Bonn B, which coincides with the $\frac{2}{3}-\frac{1}{3}$ rule approximation. The situation is totally different for polarization observables. There CIB in the ^3P states can be clearly seen. We display in Fig. 7 the analyzing powers for the breakup configurations of Figs. 1–6. The three theoretical curves correspond to the original Bonn B, to a restriction to $T=\frac{1}{2}$ with effective t operators in ^3P states, and to the inclusion of $T=\frac{3}{2}$ states. All three curves are based on a full treatment of CIB in the state $^1S_0$. That latter sophistication is, however, unimportant, since the $^1S_0$ force has little influence on A_y.

V. EFFECTS OF CHARGE-INDEPENDENCE BREAKING IN ELASTIC Nd SCATTERING

Studies of CIB in elastic Nd scattering is important for various reasons. From elastic Nd scattering one may obtain new information about $2N$ forces, which is not possible (or difficult) to obtain from the $2N$ systems. We showed in Ref. 27 that the nucleon to nucleon polarization transfer coefficient $K_y^{y'}$ for Nd scattering exhibits a strong sensitivity to the $^3S_1$-$^3D_1$ tensor force which, up to now, is insufficiently determined by two-nucleon observables only. In extracting information from $K_y^{y'}$ about the tensor force, it is important to reliably control the dependence of $K_y^{y'}$ on $^1S_0$ and ^3P $2N$ forces, which—though much weaker—is also present. Therefore, CIB in these force components should be checked. In the case of the analyzing power A_y in Nd scattering, we found that a persistent discrepancy between theory and experiment at energies below ≈ 50 MeV could be removed by introducing CIB in ^3P $2N$ forces. Therefore, it is important to know how far the $T=\frac{3}{2}$ admixture is quantitatively important and also how far the proper treatment of CIB in the $^1S_0$ is relevant.

The solution of the $3N$ equations (2.35) at 13.0 and 22.7 MeV revealed the following results. We studied the differential cross section, the nucleon and deuteron vector analyzing powers, the deuteron tensor analyzing powers, the various nucleon to nucleon and nucleon to deuteron polarization transfer coefficients. Among them there is none which is measurably sensitive to CIB in the state $^1S_0$. As an example demonstrating the weak sensitivity, in Fig. 8 we show $K_y^{y'}$ at 22.7 MeV. As for the breakup

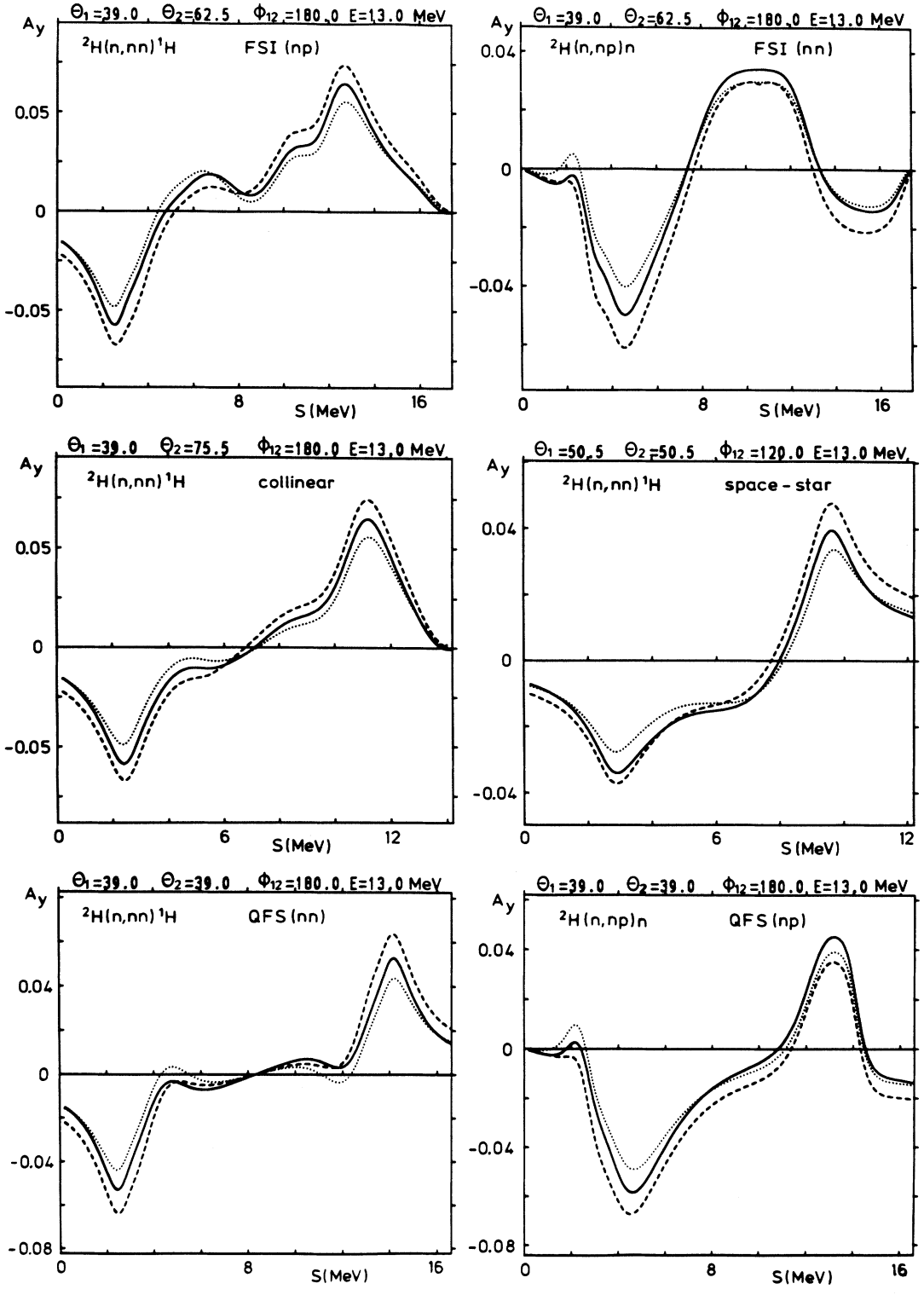

FIG. 7. The analyzing power A_y as a function of arc length S for the same configurations as in Figs. 1–6. The dotted curve is the Bonn B potential prediction with $j \leq 3$. The predictions with CIB in ^3P states as given by the modified pp and np potentials from Table II and treated exactly including $T=\frac{3}{2}$ states or approximately by the $\frac{2}{3}$-$\frac{1}{3}$ rule ($T=\frac{1}{2}$) are presented by dashed and continuous curves, respectively. All three curves are based on a full treatment of CIB in the $^1S_0$ state with Bonn B (pp) and Bonn B (np) $^1S_0$ potentials.

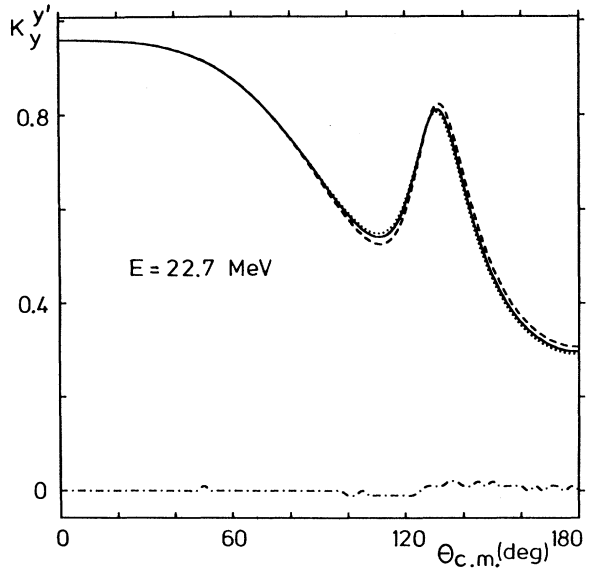

FIG. 8. The spin-transfer coefficient $K_y^{y'}$ at 22.7 MeV. Dotted and dashed curves are Bonn B potential ($j \leq 3$) predictions using Bonn B (pp) and Bonn B (np) $^1S_0$ forces, respectively. The continuous curve results in the $T=\frac{1}{2}$ approximation ($\frac{2}{3}$-$\frac{1}{3}$ rule) for the $^1S_0$ dynamic. The dash-dotted curve is the difference between this approximation and exact treatment including the $T=\frac{3}{2}$ states multiplied by 100.0.

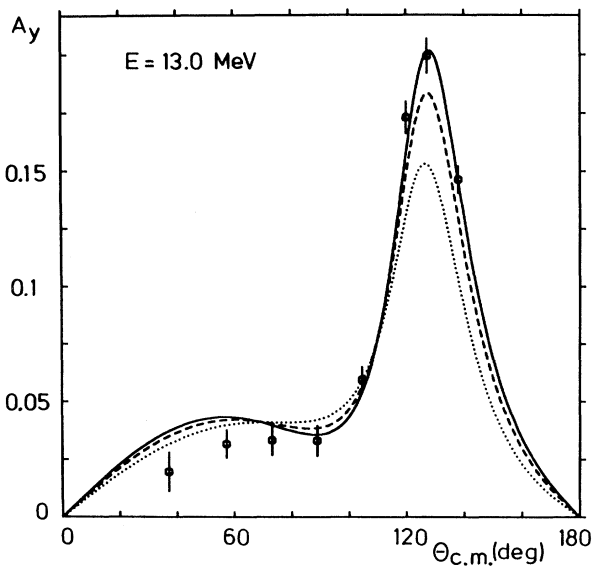

FIG. 9. The nd analyzing power A_y at 13.0 MeV. The experimental data are from Ref. 28. The dotted curve is the Bonn B calculation with $j \leq 3$. Modified, in the ^3P states, Bonn B potential predictions are given by solid and dashed curves for the nd and pd systems, respectively.

processes, four calculations are displayed: the restriction to $T=\frac{1}{2}$ working with t_{eff}, the pure Bonn B (np) and Bonn B (pp) potential predictions, and the exact inclusion of the $T=\frac{3}{2}$ states. We see that the deviations between the $T=\frac{1}{2}$ (t_{eff}) calculation and the pure Bonn B potential predictions are, at most, $\sim 3\%$ and that the $T=\frac{3}{2}$ admixture is totally negligible. For $K_y^{y'}$ the $T=\frac{1}{2}$ approximation with t_{eff} accounts perfectly well for the weak CIB in the $^1S_0$ state.

A corresponding study was performed for CIB in ^3P $2N$ forces. No observable was found in which the full calculation including the $T=\frac{3}{2}$ states was found to be necessary. However, the $3N$ observables known to be sensitive to ^3P $2N$ forces, namely, the analyzing power A_y and various nucleon to deuteron spin-transfer coefficients, show a significant difference between the $T=\frac{1}{2}$ (t_{eff}) treatment and the pure potential predictions. In Fig. 9 we show the most prominent example, A_y, at $E_n^{\text{lab}}=13.0$ MeV. The results obtained assuming CIB in ^{3}P states as given by the modified nn and np Bonn B potentials from Table II agree very well with the nd data.[28] In contrast, the pure Bonn B potential prediction deviates strongly from the data. Also shown is the prediction for the pd system.

In view of expected future measurements, we mention that, for $K_x^{x'y'}$ at 22.7 MeV, the positive maximum around $\sim 120°$ lies about 14% higher in the $T=\frac{1}{2}$ (t_{eff}) treatment than for the pure Bonn B potential predictions.

Finally, in view of the importance of $K_y^{y'}$ to the insight into the $^3S_1$-$^3D_1$ force we would like to mention its sensitivity at 22.7 MeV to CIB in ^3P $2N$ forces. While the weakening of the $^3S_1$-$^3D_1$ tensor force moves the minimum of $K_y^{y'}$ downward towards the experimental data, the CIB in ^3P 2NF introduced in Ref. 10 shifts the minimum upward by about 2%; so it keeps various dynamical effects separated.

VI. CONCLUSION

CIB and CSB of $2N$ forces are visible in $3N$ observables. In the context of the generalized Pauli principle introducing isospin degrees of freedom, the difference between the nn, pp, and np forces is reflected by an admixture of the $T=\frac{3}{2}$ states to the dominant $T=\frac{1}{2}$ states. For the modified AGS equations, which we are using for our $3N$ scattering calculations, we explicitly demonstrated the equivalence of that isospin formalism (with the inclusion of the $T=\frac{1}{2}$ and $\frac{3}{2}$ states) to a treatment which regards neutrons and protons to be distinguishable particles. Even if the $T=\frac{3}{2}$ admixture can be neglected, effects of isospin violation may still be noticeable and will then be taken into account by an effective t operator ($\frac{2}{3}$-$\frac{1}{3}$ rule), as has been noticed before.[7–9] We applied these formal insights in realistic $3N$ calculations with the meson-theoretical $2N$ potentials of the Paris and Bonn groups. For the triton we illustrated CIB in the $^1S_0$ $2N$ force, which brings the Bonn B and Paris potential predictions for the triton binding energy closer together. Extending our triton code to include $T=\frac{3}{2}$ states, we found that CIB in the $^1S_0$ two-nucleon force changes the binding energy only by ~ 1 keV which is negligible in comparison to the still existing discrepancy to the experi-

mental value. CIB and CSB, as introduced in Ref. 10 for the ^3P 2NF have a small effect of ~ 30 keV and reduces the binding-energy difference between ^{3}H and ^{3}He by 10 keV.

For $3N$ scattering we studied breakup and elastic Nd scattering processes. Among the investigated breakup configurations, the FSI cross sections were most sensitive to CIB in the $^1S_0$ 2NF. A proper treatment requires the inclusion of the $T=\frac{3}{2}$ states to clearly distinguish the *nn* and *np* forces. The effective t operator of Eq. (1.1), keeping alone $T=\frac{1}{2}$, is not sufficient in the FSI peak area; it is, however, a good approximation for the *nn* QFS. Other breakup configurations, such as the space star, collinearity, and *np* QFS, turned out to be insensitive to CIB. Very small effects of CIB in ^3P 2NF were visible in FSI and *np* QFS cross sections.

Strong and significant shifts showed up in the analyzing powers for all the considered breakup configurations, if CIB in ^3P 2NF was introduced.

Spin observables in elastic scattering are, in general, insensitive to CIB in $^1S_0$ and ^3P 2NF. Interesting exceptions are the vector analyzing powers and nucleon to deuteron spin-transfer coefficients. They show a strong sensitivity to ^3P 2NF and exhibit clear effects of CIB in these 2NF components. We illustrated that for the CIB in ^3P 2NF, introduced in Ref. 10 to explain low energy A_y's in the *nd* and *pd* systems. In that case, the neglect of a $T=\frac{3}{2}$ admixture turned out to be justified.

The numerical progress in solving $3N$ equations and new experimental data of high quality make the study of CIB in $3N$ scattering possible and useful. Future applications to FSI's and to nucleon to deuteron spin-transfer coefficients appear promising.

ACKNOWLEDGMENTS

This work was supported financially by the Deutsche Forchungsgemeinschaft (H.W.) and by the Bundesministerium für Forschung und Technologie (H.K.). The numerical work was performed on the CRAY Y-MP of the Höchstleistungsrechenzentrum in Jülich.

APPENDIX

To derive (2.58) from (2.35) we start from

$$\langle nnp|T|\Phi\rangle=\langle nnp|tP|\Phi\rangle+\langle nnp|tPG_0T|\Phi\rangle \ . \tag{A1}$$

Using (2.43) and manipulating permutation operators, one finds

$$\begin{aligned}\langle nnp|T|\Phi\rangle=&t_{nn}^{t=1}(23)(\hat{P}_{12}-\hat{P}_{13})\hat{P}_0|\hat{\Phi}\rangle\frac{1}{\sqrt{2}}\\&+t_{nn}^{t=1}(23)G_0(\hat{P}_{12}\hat{P}_{23}\langle npn|T|\Phi\rangle\\&+\hat{P}_{13}\hat{P}_{23}\langle pnn|T|\Phi\rangle) \ .\end{aligned} \tag{A2}$$

Next we apply the cyclical permutation $\hat{P}_{13}\hat{P}_{23}$ and get

$$\begin{aligned}\hat{P}_{13}\hat{P}_{23}\langle nnp|T|\Phi\rangle=&\frac{1}{\sqrt{2}}t_{nn}^{t=1}(12)(1-\hat{P}_{12})\hat{P}_0|\hat{\Phi}\rangle\\&+t_{nn}^{t=1}(12)G_0\\&\times(\langle npn|T|\Phi\rangle\\&+\hat{P}_{13}\hat{P}_{12}\langle pnn|T|\Phi\rangle) \ .\end{aligned} \tag{A3}$$

Using $\hat{P}_{13}\hat{P}_{12}=\hat{P}_{12}\hat{P}_{23}$ and (2.52) led to (2.58).

*Permanent address: Institute of Physics, Jagellonian University, PL 30059 Cracow, Poland.

[1]O. Schori *et al.*, Phys. Rev. C **35**, 2252 (1987); G. F. de Teramond and B. Gabioud, *ibid.* **36**, 691 (1987).
[2]R. A. Arndt *et al.*, Phys. Rev. D **35**, 128 (1987).
[3]V. G. J. Stoks *et al.*, Phys. Rev. Lett. **61**, 1702 (1988).
[4]W. Schuster, Habilitationsschrift, Erlangen, 1989.
[5]W. M. Kloet and J. A. Tjon, Ann. Phys. (N.Y.) **79**, 407 (1973); A. Bömelburg, W. Glöckle, and W. Meier, in *Few-Body Problems in Physics,* edited by B. Zeitnitz (Elsevier, Amsterdam, 1984), Vol. II, p. 483.
[6]W. Glöckle, H. Witala, and Th. Cornelius, Nucl. Phys. **A508**, 115C (1990); Proceedings of the 25th Zakopane School on Physics, Zakopane, 1990 (World-Scientific, Singapore, in press), and references therein.
[7]H. Witała, W. Glöckle, and Th. Cornelius, Phys. Rev. C **39**, 384 (1989).
[8]D. J. Klepacki, Y. E. Kim, and R. A. Brandenburg, Phys. Rev. C **38**, 998 (1988).
[9]J. L. Friar, B. F. Gibson, and G. L. Payne, Phys. Rev. C **36**, 1140 (1987).
[10]H. Witała and W. Glöckle, Nucl. Phys. A (in press).
[11]W. Glöckle, *The Quantum Mechanical Few-Body Problem,* Vol. 273 of *Lecture Notes in Physics* (Springer-Verlag, Berlin, 1983), p. 3.
[12]E. O. Alt, P. Grassberger, and W. Sandhas, Nucl. Phys. **B2**, 167 (1967).
[13]R. T. Cahill and I. H. Sloan, Nucl. Phys. **A165**, 16 (1971).
[14]M. Lacombe *et al.*, Phys. Rev. C **21**, 861 (1980).
[15]R. Machleidt, Adv. Nucl. Phys. **19**, 189 (1989).
[16]M. M. Nagels, T. A. Rijken, and J. J. de Swart, Phys. Rev. D **17**, 768 (1978).
[17]R. B. Wiringa, R. A. Smith, and T. A. Ainsworth, Phys. Rev. C **29**, 1207 (1984).
[18]R. V. Reid, Ann. Phys. (N.Y.) **50**, 411 (1968).
[19]T. Sasakawa and E. Hadjimichael, Nucl. Phys. **A508**, 161C (1990).
[20]W. Glöckle, Nucl. Phys. **A381**, 343 (1982); A. Bömelburg, Phys. Rev. C **28**, 403 (1983); **34**, 14 (1986).
[21]J. L. Friar, B. F. Gibson, and G. L. Payne, Phys. Rev. C **37**, 2869 (1988).
[22]W. Meier and W. Glöckle, Phys. Lett. **138B**, 329 (1984).
[23]K. M. Watson, Phys. Rev. **88**, 1163 (1952); A. B. Migdal, Zh. Eksp. Teor. Fiz. **28**, 3 (1954) [Sov. Phys. JETP **1**, 2 (1955)]; M. C. Goldberger and K. M. Watson, *Collision Theory* (Wiley, New York, 1964), p. 540.
[24]H. Witała, Th. Cornelius, and W. Glöckle, Few-Body Syst. **5**, 89 (1988).
[25]J. Strate *et al.*, Nucl. Phys. **A501**, 51 (1989).
[26]M. Stephan *et al.*, Phys. Rev. C **39**, 2133 (1989).
[27]M. Clajus *et al.*, Phys. Lett. B **245**, 333 (1990).
[28]J. Cub *et al.*, Few-Body Syst. **6**, 151 (1989).